Nonlinear Attitude Motion of a Dual-Spin Spacecraft Containing Spherical Dampers

P.K. Winfree* and J.E. Cochran Jr.†
Auburn University, Auburn, Alabama

The generalized method of averaging is used in an investigation of the nonlinear attitude motion of a symmetric dual-spin spacecraft containing two spherical dampers, arbitrarily located on the rotor and platform (one damper on each). The spherical dampers are intended to represent fully filled fuel tanks. The motions of the dampers are treated as sources of perturbations of the externally torque-free attitude motion and approximate attitude motion equations are obtained that are valid through first order in the ratios of the damper moments of inertia to the spacecraft transverse moment of inertia. The generalized method of averaging is used to find an approximate averaged differential equation for the nutation angle which is used to investigate the stability of the attitude motion in the case of a constant-speed rotor when the nutation angle is small and large. For the case of a free rotor, averaged equations for the nutation angle and the symmetry axis component of the rotor angular momentum are used to show that "stability reversal" may occur due to varying relative spin rate of the rotor.

Nomenclature

$[A]$ = transformation matrix, inertial reference frame to platform-fixed reference frame
a_{ij} = the ijth element of $[A]$
C_P = platform damping coefficient
C_R = rotor damping coefficient
$CXYZ$ = inertially fixed reference frame
$Cx_1x_2x_3$ = platform-fixed reference frame
$\hat{e}_1, \hat{e}_2, \hat{e}_3$ = platform-fixed unit vector triad
H_1, H_2, H_3 = platform-fixed components of the spacecraft rotational angular momentum
h = symmetry axis component of the rotor's angular momentum when $I_R = 0$
h_i $= h_{P_i} + h_{R_i}, \quad i = 1,2,3$
h_{P1}, h_{P2}, h_{P3} = platform-fixed components of the platform damper's angular momentum
h_{R1}, h_{R2}, h_{R3} = platform-fixed components of the rotor damper's angular momentum
I_P = moment of inertia of the platform damper
I_R = moment of inertia of the rotor damper
I_S^* $= J_P + J_R + I_P + I_R$
I_t = transverse moment of inertia of the spacecraft (excluding dampers)
I_t^* $= I_t + I_P + I_R$
J_P = spin axis moment of inertia of the platform (excluding dampers)
J_R = spin axis moment of inertia of the rotor (excluding damper)
J_t = transverse moment of inertia of the rotor (excluding damper)
k_{P1}, k_{P2}, k_{P3} = inertial components of the platform damper's angular momentum
k_{R1}, k_{R2}, k_{R3} = inertial components of the rotor damper's angular momentum
M_1, M_2, M_3 = components of external moment
r_3 = symmetry axis component of rotor angular momentum
T_{P1}, T_{P2}, T_{P3} = components of torque on the platform dampers
T_{R1}, T_{R2}, T_{R3} = components of torque on the rotor dampers
t = time
$x = x_1$ $= \cos\Theta$
x_2 $= [h + I_R(\omega_3 + \dot{\phi})]/H$
z $= \sin\Theta$
α $= I_P/I_t = I_R/I_t$, small parameter
δ_P $= C_P/I_P$
δ_R $= C_R/I_R$
Θ = nutation angle
Λ = frequency parameter, $H_3(1/J_P - 1/I_t) - h/J_P$
λ = frequency parameter, H/I_t
μ_P $= \delta_P\lambda/(\delta_P^2 + \lambda^2)$
μ_R $= \delta_R\lambda/(\delta_R^2 + \lambda^2)$
ρ $= J_P/I_t$
σ $= J_R/I_t$
Φ = angle of proper rotation
$\dot{\phi}$ = angular speed of the rotor with respect to the platform
Ψ = precession angle
Ω = constant angular speed of a driven rotor with respect to the platform (constant-speed rotor)
$\underline{\Omega}_R$ = angular velocity of the rotor with respect to the platform
$\omega_1, \omega_2, \omega_3$ = platform-fixed components of the spacecraft angular velocity
$\omega_{P1}, \omega_{P2}, \omega_{P3}$ = components of the angular velocity of platform damper wrt its housing
$\omega_{R1}, \omega_{R2}, \omega_{R3}$ = components of the angular velocity of the rotor damper wrt its housing

Other Notation

$[\ ]$ = square matrix
$\{\ \}$ = column matrix of vector components
$(\dot{\ })$ = time rate of change of the elements of ( )
$(\bar{\ })$ = average value of ( )
$\mathcal{O}(\ )$ = of order ( )

Presented as Paper 84-2019 at the AIAA/AAS Astrodynamics Conference, Seattle, WA, Aug. 20–22, 1984; received Jan. 18, 1985; revision received Feb. 5, 1986.

*Graduate Student (presently First Lieutenant, USAF, Vandenberg AFB, CA). Member AIAA.

†Professor of Aerospace Engineering. Associate Fellow AIAA.

Introduction

SPACECRAFT containing spinning rotors and nominally despun platforms are called "dual-spin" spacecraft. In such a dual-spin configuration, the rotor provides gyroscopic stiffness for stability, while the despun platform provides an oriented platform that usually contains scientific instruments, antennas, solar panels, and other components which must be oriented in a "fixed" direction.

A classical rigid-body analysis of the attitude stability of a spinning single-body spacecraft indicates that a state of steady spin of the spacecraft is stable if the rotation is about its principal axis of either minor or major moment of inertia. This classic stability criterion has been known to be inadequate since 1958, when the unanticipated instability of motion about the minor spin axis of the first U.S. satellite, Explorer I, was observed. The explanation of this instability is credited to Bracewell and Garriott in Ref. 1, who modeled Explorer I as a semirigid body that dissipated energy and, therefore, would approach the state of minimum energy corresponding to the rotation about its axis of the maximum moment of inertia.

In 1964, Landon and Stewart[2] demonstrated that the motion of the spin axis of a symmetric dual-spin spacecraft with a despun platform may be stable if the spin axis of either the maximum or minimum moments of inertia, provided an energy dissipation device is placed on the despun platform. In an independent development of the dual-spin stabilization concept, Iorillo[3] extended the scope of analysis to axisymmetric dual-spin vehicles with energy dissipating mechanisms, "dampers," on both the rotor and platform. This extension allowed for the analysis of spacecraft of realistic complexity, since, in reality, the internal motion on both the rotor and platform cause energy dissipation.

Although the problem of attitude stability of dual-spin spacecraft has been studied for more than two decades, it continues to be an area in which more can be learned. Several different methods can be used to study the attitude motion of a specific spacecraft, but if the type of configuration permits, a conventional linear stability analysis is a convenient first step. A linear stability analysis of a specific dual-spin spacecraft containing arbitrarily located spherical dampers has been presented by Laskin, et al.[4] They also obtained corroborative results using an energy-sink method. In applying both methods, small nutation angles were assumed. An alternative approach to the usual energy-sink method is available, since when the energy dissipation is slow enough to justify the use of an energy-sink method, a perturbation method may be often used effectively. An analysis of this type was used by Cochran and Shu[5] to analyze the nutational motion of a different spacecraft configuration and they obtained very good results.

The model considered in Ref. 4 is of the "ideal" type for analysis because it is axisymmetric and the energy dissipating devices on the rotor and platform are such that energy can be dissipated without changes in the inertia properties of the spacecraft. However, because the spacecraft attitude motion is nonlinear, linear analysis does not, and cannot be expected to, predict correctly the attitude stability of the spacecraft with respect to substantial perturbations in initial conditions. Laskin, et al. also found, via simulation on a digital computer, that in some cases the stability is dependent upon the ratio of the spacecraft's axial and transverse moments of inertia, a parameter that does not appear in the linearized equations of Ref. 4.

This paper presents a "perturbation analysis" of the attitude motion of the type of spacecraft investigated in Ref. 4. Following to some extent Cochran and Shu,[5] the effects of the motions of the spherical bodies are treated as perturbations of the attitude motion. The platform-fixed components of the total angular momentum of the spacecraft are first used as dependent variables along with the components of angular momenta of the dampers and the rotor's spin axis angular momentum. Euler angles defining the attitude of the platform are then used to make a change of variables and the zero-order solutions for damper motions are used to obtain equations in the "normal form" required to apply the generalized method of averaging.[6,7]

The generalized method of averaging is used to obtain an approximate differential equation for the "averaged" nutation angle of the spacecraft when the rotor is spinning at a constant speed with respect to the platform. This equation contains all of the spacecraft inertia and damping parameters and is used to determine the regions of stable and unstable spacecraft attitude motion (in the sense of "nutation") in the damping parameter plane for several sets of spacecraft inertia parameters. Results obtained using the exact solution for the "averaged" nutation angle are also compared to those found by numerically integrating the full set of nonlinear equations. The effects of a free rotor on the attitude motion of the spacecraft are then addressed. When the rotor is free, an equation governing the rotor spin rate is needed, in addition to an equation for the nutational motion. The two coupled equations provide a stability criterion. Results are presented explaining the "stability reversal" observed in some of the numerical results of Ref. 4 for large nutation angles.

Spacecraft Model

The type of spacecraft considered in this paper is a symmetric dual-spin configuration such as that depicted in Fig. 1. The physical model of this type spacecraft consists of two axisymmetric rigid bodies, a nominally despun platform, and a rapidly spinning rotor. Both the platform and rotor contain arbitrarily located spherical dampers. These dampers may be thought of as fully filled fuel tanks that are modeled as rigid spheres with constant surface damping coefficients.[4] Energy dissipation that occurs when the spherical dampers rotate with respect to their respective containers is assumed to be due to the viscous torques. The spherical nature of the dampers allows for energy dissipation with no change in the inertia properties of the spacecraft.

In Fig. 1, the $Cx_1x_2x_3$ coordinate system has its origin at the center of mass of the spacecraft and rotates with the platform. The unit vector triad $(\hat{e}_1, \hat{e}_2, \hat{e}_3)$ is attached to $Cx_1x_2x_3$. The angular velocity of the rotor with respect to the platform is $\boldsymbol{\Omega}_R = \dot{\phi}\hat{e}_3$.

The centroidal transverse moment of inertia of the spacecraft is I_t; the moments of inertia of the platform and rotor about their axes of symmetry are J_P and J_R, respectively. The spherical bodies have moments of inertia I_P (platform) and I_R (rotor). The angular velocity component of the platform in the $\hat{e}_j$ direction is ω_j, while those of the spherical bodies with respect to their housings are ω_{Pj} (platform) and ω_{Rj} (rotor).

In this analysis, the translational motion of the spacecraft is considered to be uncoupled from its attitude motion, which is assumed to be torque-free.

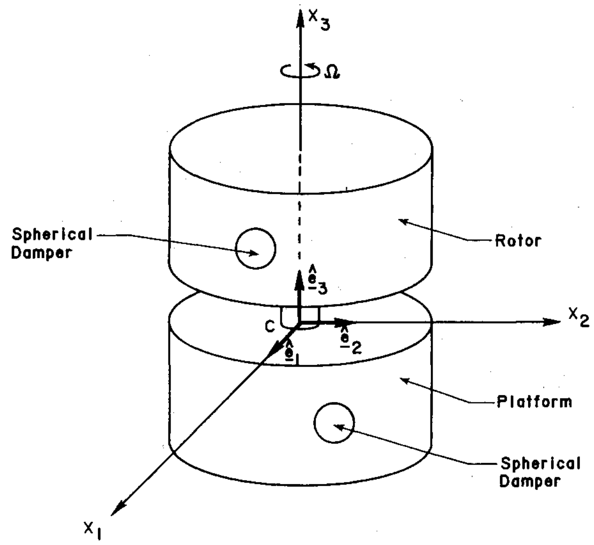

Fig. 1 Spacecraft configuration.

Equations for Use in the Generalized Method of Averaging

Attitude Motion of the Spacecraft

The equations for the attitude motion of the spacecraft may be developed in terms of $\boldsymbol{H}$, the angular momentum of the system. The platform-fixed components of $\boldsymbol{H}$ are

$$H_1 = I_t\omega_1 + I_P(\omega_{P1} + \omega_1) + I_R(\omega_{R1} + \omega_1) \tag{1a}$$

$$H_2 = I_t\omega_2 + I_P(\omega_{P2} + \omega_2) + I_R(\omega_{R2} + \omega_2) \tag{1b}$$

$$H_3 = J_P\omega_3 + J_R(\omega_3 + \dot{\phi}) + I_P(\omega_{P3} + \omega_3) + I_R(\omega_{R3} + \omega_3 + \dot{\phi}) \tag{1c}$$

The angular momenta of the dampers have platform-fixed components,

$$h_{Pi} = I_P(\omega_{Pi} + \omega_i), \quad \text{for } i = 1,2,3 \tag{2a}$$

$$h_{Ri} = I_R(\omega_{Ri} + \omega_i), \quad \text{for } i = 1,2 \tag{2b}$$

$$h_{R3} = I_R(\omega_{R3} + \omega_3 + \dot{\phi}) \tag{2c}$$

Hence, Eqs. (1) may be rewritten as

$$H_1 = I_t\omega_1 + h_{P1} + h_{R1} \tag{3a}$$

$$H_2 = I_t\omega_2 + h_{P2} + h_{R2} \tag{3b}$$

$$H_3 = J_P\omega_3 + h_{P3} + h_{R3} + h \tag{3c}$$

where $h = J_R(\omega_3 + \dot{\phi})$ is the symmetry axis component of the rotor's angular momentum when $I_R = 0$.

If the angular momentum components of the platform and rotor dampers are combined into single terms, i.e.,

$$\{h_i\} = \{h_{Pi}\} + \{h_{Ri}\}, \text{for } i = 1,2,3 \tag{4}$$

then we may write the following expressions for ω_1, ω_2, and ω_3:

$$\omega_1 = (H_1 - h_1)/I_t \tag{5a}$$

$$\omega_2 = (H_2 - h_2)/I_t \tag{5b}$$

$$\omega_3 = (H_3 - h - h_3)/J_P \tag{5c}$$

The equation of motion for the spacecraft as a whole is

$$\boldsymbol{M} = \mathring{\boldsymbol{H}} + \boldsymbol{\omega} \times \boldsymbol{H} \tag{6}$$

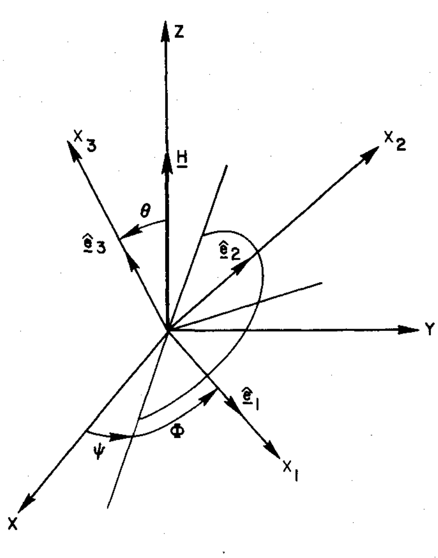

Fig. 2 Euler angles.

where, $\mathring{\boldsymbol{H}}$ is the time rate of change of $\boldsymbol{H}$ as seen in the $Cx_1x_2x_3$ system and $\boldsymbol{M}$ the external torque about the spacecraft's center of mass. Since the motion of the spacecraft is considered torque-free, the following matrix equation may be obtained from Eq. (6):

$$\{\dot{H}\} = -[\tilde{\omega}]\{H\} \tag{7}$$

where $\{\dot{H}\} = [\dot{H}_1 \dot{H}_2 \dot{H}_3]^T$ and

$$[\tilde{\omega}] = \begin{bmatrix} 0 & -\omega_3 & \omega_2 \\ \omega_3 & 0 & -\omega_1 \\ -\omega_2 & \omega_1 & 0 \end{bmatrix} \tag{8}$$

Equation (7) may be expanded using Eqs. (5) to obtain

$$\dot{H}_1 = H_2\left[H_3\left(\frac{1}{J_P} - \frac{1}{I_t}\right) - \frac{h}{J_P}\right] - \frac{H_2h_3}{J_P} + \frac{H_3h_2}{I_t} \tag{9a}$$

$$\dot{H}_2 = -H_1\left[H_3\left(\frac{1}{J_P} - \frac{1}{I_t}\right) - \frac{h}{J_P}\right] + \frac{H_1h_3}{J_P} - \frac{H_3h_1}{I_t} \tag{9b}$$

$$\dot{H}_3 = \frac{H_2h_1}{I_t} - \frac{H_1h_2}{I_t} \tag{9c}$$

If we let

$$\Lambda = H_3\left(\frac{1}{J_P} - \frac{1}{I_t}\right) - \frac{h}{J_P} \tag{10}$$

Eqs. (7) may be rewritten as

$$\dot{H}_1 = H_2\Lambda - \frac{H_2h_3}{J_P} + \frac{H_3h_2}{I_t} \tag{11a}$$

$$\dot{H}_2 = -H_1\Lambda + \frac{H_1h_3}{J_P} - \frac{H_3h_1}{I_t} \tag{11b}$$

$$\dot{H}_3 = \frac{H_2h_1}{I_t} + \frac{H_1h_2}{I_t} \tag{11c}$$

Now, we consider Fig. 2 which shows the fixed reference frame $CXYZ$ with the constant angular momentum vector $\boldsymbol{H}$ aligned with the Z axis. The spacecraft axis system $Cx_1x_2x_3$ is obtained from the $CXYZ$ system by a 3-1-3 sequence of rotations through the Euler angles Ψ, Θ, and Φ. These Euler angles may be used to construct the transformation matrix,

$$[A] = \begin{bmatrix} c\Phi & s\Phi & 0 \\ -s\Phi & c\Phi & 0 \\ 0 & 0 & 1 \end{bmatrix} \begin{bmatrix} 1 & 0 & 0 \\ 0 & c\Theta & s\Theta \\ 0 & -s\Theta & c\Theta \end{bmatrix} \begin{bmatrix} c\Psi & s\Psi & 0 \\ -s\Psi & c\Psi & 0 \\ 0 & 0 & 1 \end{bmatrix} \tag{12}$$

where $c \triangleq$ cosine and $s \triangleq$ sine.

Since $\boldsymbol{H}$ is collinear with the Z axis, the platform-fixed components of $\boldsymbol{H}$ are

$$H_1 = H\sin\Theta\sin\Phi \tag{13a}$$

$$H_2 = H\sin\Theta\cos\Phi \tag{13b}$$

$$H_3 = H\cos\Theta \tag{13c}$$

By differentiating Eqs. (13) with respect to time and using Eqs. (11) and (13), we obtain equations for the nutation angle and angle of proper rotation, viz.,

$$\dot{\Theta} = \frac{h_2}{I_t}\sin\Phi - \frac{h_1}{I_t}\cos\Phi \tag{14a}$$

and

$$\dot{\Phi} = \Lambda - \frac{h_3}{J_P} + \frac{h_1 \sin\Phi + h_2 \cos\Phi}{I_t \tan\Theta} \tag{14b}$$

These are two attitude equations that will be used later in applying the generalized method of averaging. A third equation for the precession angle of the platform can be obtained from Fig. 2 and Eqs. (5).

Since $\dot{\Psi} = (\omega_1 \sin\Phi + \omega_2 \cos\Phi)/\sin\Theta$,

$$\dot{\Psi} = \frac{[(H_1 - h_1)/I_t]\sin\Phi + [(H_2 - h_2)/I_t]\cos\Phi]}{\sin\Theta} \tag{15}$$

At this point, we assume that each of the damper inertias is much smaller than I_t. Since h_i contains I_P and I_R, we may write

$$\dot{\Theta} = \mathcal{O}(\alpha) \tag{16a}$$

$$\dot{\Phi} = \Lambda + \mathcal{O}(\alpha) \tag{16b}$$

$$\dot{\Psi} = \lambda + \mathcal{O}(\alpha) \tag{16c}$$

where $\lambda = H/I_t$ and $\mathcal{O}(\alpha)$ indicates terms of order $\alpha_P = I_P/I_t$ and/or $\alpha_R = I_R/I_t$.

By using $h = J_R(\omega_3 + \dot{\phi})$ and Eq. (5c), we find that

$$h = [J_R/(J_P + J_R)]H_3 + [J_P J_R(J_P + J_R)]\dot{\phi} + \mathcal{O}(\alpha)$$

Thus, to zeroth order in α, Λ is constant when $\dot{\phi}$ is constant, i.e., when the rotor is driven at constant speed with respect to the platform.

If, on the other hand, the rotor is free, h is constant when $I_R = 0$ because then it is the symmetry axis component of the rotor angular momentum. Hence, the *zeroth-order* approximations to Θ, Φ, and Ψ are

$$\Theta = \Theta_0 \tag{17a}$$

$$\Phi = \Lambda t + \Phi_0 \tag{17b}$$

$$\Psi = \lambda t + \Psi_0 \tag{17c}$$

where Θ_0, Φ_0, and Ψ_0 are the initial conditions. Furthermore, Eqs. (14) and (15) may be put into normal form, to *first-order*, if appropriate *zeroth-order* approximations for the h_i may be found.

Attitude Motion of the Platform Damper

To develop the solutions for the platform damper attitude motion in the desired form, it is convenient to use the *inertial* components of angular momentum. If $\{k_P\}$ is used to denote the matrix of inertial components of the angular momentum vector of the platform damper, then by using the transformation matrix $[A]$ given by Eq. (12),

$$\{h_P\} = [A]\{k_P\} \tag{18}$$

The vector form of the equation of motion for the platform damper is

$$\mathring{\boldsymbol{h}}_P + \boldsymbol{\omega} \times \boldsymbol{h}_P = -C_P \boldsymbol{\omega}_P \tag{19}$$

By writing Eq. (19) in matrix form and substituting $\{\omega_P\} = (1/I_P)\{h_P\} - \{\omega\}$, we may obtain the result

$$\{\dot{h}_P\} = -\frac{C_P}{I_P}\{h_P\} + C_P\{\omega\} - [\tilde{\omega}]\{h_P\} \tag{20}$$

In the zeroth-order approximation, Eq. (20) is a nonhomogeneous, linear, ordinary differential equation with variable coefficients, since $[\tilde{\omega}]$ is time varying. However, because of the sphericity of the dampers, we can transform $\{h_P\}$, and hence Eq. (20), into inertially fixed components. Since, from Eq. (18),

$$\{\dot{h}_P\} = [\dot{A}]\{k_P\} + [A]\{\dot{k}_P\} \tag{21}$$

and since $[\dot{A}] = -[\tilde{\omega}][A]$, it follows that

$$\{\dot{k}_P\} = -\delta_P\{k_P\} + I_P\delta_P[A]^T\{\omega\} \tag{22}$$

where $\delta_P = C_P/I_P$. We note that Eq. (22) is exact.

For convenience, let

$$\{k_P\} = \{a_P\}e^{-\delta_P t} \tag{23}$$

and get

$$\{\dot{a}_P\} = C_P e^{\delta_P t}[A]^T\{\omega\} \tag{24}$$

Since we are seeking a *zeroth-order* solution for $\{h_p\}$, we may substitute the zeroth-order approximations to $[\dot{A}]$ and $\{\omega\}$ (see Appendix) into Eq. (24) and formally integrate with respect to time as it appears explicitly. The elements of $\{a_P\}$ found in this manner are

$$a_{P1} = \frac{C_P\Lambda z}{\delta_P^2 + \lambda^2}\{e^{\delta_P t}(\delta_P \sin\Psi - \lambda\cos\Psi) + \lambda\} a_{P10} \tag{25a}$$

$$a_{P2} = \frac{-C_P\Lambda z}{\delta_P^2 + \lambda^2}\{e^{\delta_P t}(\delta_P \cos\Psi + \lambda\sin\Psi) - \delta_P\} + a_{P20} \tag{25b}$$

$$a_{P3} = I_P\left[\frac{\lambda z^2 + x(H_3 - h)}{J_P}\right](e^{\delta_P t} - 1) + a_{P30} \tag{25c}$$

and a_{Pj0} is the initial value of a_{Pj} where $x \triangleq \cos\Theta$ and $z \triangleq \sin\Theta$. When used in Eq. (23), the above expressions give the approximate inertial components of the platform damper angular momentum as functions of time and the fast variable Ψ. [Note that Φ does not appear in Eqs. (25). The absence of Φ is due to the symmetry of the spacecraft.] These components may be transformed into platform-fixed components. After performing some nontrivial algebra and neglecting transient terms, we find that

$$h_{P1} = \frac{C_P z\Lambda}{\delta_P^2 + \lambda^2}\left[-\lambda\cos\Phi - \frac{C_P}{\delta_P}x\sin\Phi\right] + I_P z\sin\Phi\left[\frac{\lambda z^2 + x(H_3 - h)}{J_P}\right] \tag{26a}$$

$$h_{P2} = \frac{C_P z\Lambda}{\delta_P^2 + \lambda^2}[\lambda\sin\Phi - \delta_P x\cos\Phi] + I_P z\cos\Phi\left[\lambda z^2 + \frac{x(H_3 - h)}{J_P}\right] \tag{26b}$$

$$h_{P3} = \frac{C_P^2 z^2\Lambda/I_P}{\delta_P^2 + \lambda^2} + I_P x\left[\lambda z^2 + \frac{x(H_3 - h)}{J_P}\right] \tag{26c}$$

The above expressions are zeroth-order approximations to the angular momentum components of the platform damper. They are functions of the slow variable Θ found in x and z and the fast variable Φ.

Motion of the Rotor Damper

The equations for the rotor damper motion may be developed in essentially the same manner as those for the platform. If $\{k_R\}$ denotes the inertial angular momentum, then the same transformation exists for the rotor dampers, i.e.,

$$\{h_R\} = [A]\{k_R\} \tag{27}$$

If a vector $[\dot{\phi}]$ is defined such that

$$\{\dot{\phi}\} = (0 \quad 0 \quad \dot{\phi})^T \tag{28}$$

then Eqs. (2b) and (2c) can be written in the matrix form,

$$\{h_R\} = I_R\{\omega_R\} + I_R\{\omega\} + I_R\{\dot{\phi}\} \tag{29}$$

The vector form of the equation of motion of the rotor is

$$\mathring{\boldsymbol{h}}_R + \boldsymbol{\omega} \times \boldsymbol{h}_R = \boldsymbol{T}_R \tag{30}$$

By switching to matrix notation and substituting

$$\{\omega_R\} = \frac{1}{I_R}\{h_R\} - \{\omega\} - \{\dot{\phi}\}$$

into Eq. (30), we get

$$\{\dot{h}_R\} = -\frac{C_R}{I_R}\{h_R\} + C_R\{\omega\} + C_R\{\dot{\phi}\} - [\tilde{\omega}]\{h_R\} \tag{31}$$

A procedure essentially the same as that followed to obtain the zeroth-order approximation to $\{h_P\}$ can be used to obtain an analogous approximation to $\{h_R\}$. The reader is referred to Ref. 9 for the details. The results for the platform-fixed components of the rotor damper's angular momentum are (again with transient terms neglected),

$$h_{R1} = -\left[\frac{C_R z(\Lambda + \dot{\phi})}{\delta_R^2 + \lambda^2}\right](\delta_R x \sin\Phi + \lambda\cos\Phi) + I_R z\left[\lambda z^2 + \frac{x(H_3 - h)}{J_P} + x\dot{\phi}\right]\sin\Phi \tag{32a}$$

$$h_{R2} = \left[\frac{C_R z(\Lambda + \dot{\phi})}{\delta_R^2 + \lambda^2}\right][\lambda\sin\Phi - \delta_R x\cos\Phi] + I_R z\left[\lambda z^2 + \frac{x(H_3 - h)}{J_P} + x\dot{\phi}\right]\cos\Phi \tag{32b}$$

$$h_{R3} = \left[\frac{C_R z^2\delta_R(\Lambda + \dot{\phi})}{\delta_R^2 + \lambda^2}\right] + I_R x\left[\lambda z^2 + \frac{x(H_3 - h)}{J_P} + x\dot{\phi}\right] \tag{32c}$$

Equations (32) are zeroth-order approximations to the platform-fixed components of the angular momentum of the rotor damper as functions of the slow variable Θ and the fast variable Φ.

Transformation of the Equations to Normal Form

To apply the generalized method of averaging, it is necessary to have equations of the form (see Refs. 7 and/or 9),

$$\{\dot{x}\} = \alpha\{X_1\} + \alpha^2\{X_2\} + \cdots \tag{33a}$$

$$\{\dot{y}\} = \{Y_0\} + \alpha\{Y_1\} + \alpha^2\{Y_2\} + \cdots, \tag{33b}$$

where α is a small constant, $\{x\}$ a vector of slow variables, $\{y\}$ a vector of fast variables, and the vector functions $\{X_i\}$ and $\{Y_j\}$ periodic functions in the elements of $\{y\}$ with period 2π.

To arrive at the desired normal form, we combine the zeroth-order angular momentum solutions, substitute them into Eq. (14a), and use Eq. (14b) to obtain the rather concise result,

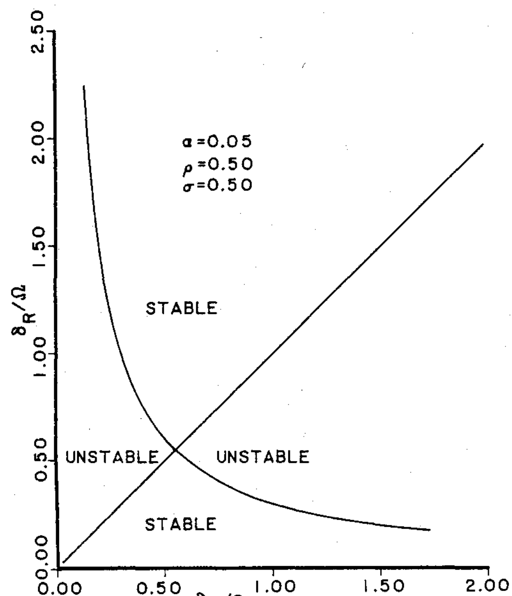

Fig. 3 Stability diagram for $\alpha = 0.05$, $\rho = 0.5$, and $\sigma = 0.5$.

$$\dot{\Theta} = z[(I_P/I_t)\mu_P\Lambda + (I_R/I_t)\mu_R(\Lambda + \dot{\phi})] \tag{34}$$

where

$$\mu_P \triangleq \delta_P\lambda/(\delta_P^2 + \lambda^2) \tag{35a}$$

$$\mu_R \triangleq \delta_R\lambda/(\delta_R^2 + \lambda^2) \tag{35b}$$

For the remainder of this paper, we will assume that $I_P = I_R$ and take $\alpha = I_P/I_t = I_R/I_t$ as our small parameter.

Because z and Λ in the above equations are functions of x, it is chosen as the slow variable. From $x = \cos\Theta$, it follows that

$$\dot{x} = -\dot{\Theta}\sin\Theta = -\dot{\Theta}z \tag{36}$$

Hence, $\dot{\Theta} = -\dot{x}/z$ and Eq. (34) may be replaced by

$$\dot{x} = -\alpha z^2[\mu_P\Lambda + \mu_R(\Lambda + \dot{\phi})] \tag{37}$$

Equation (37) is one of the desired equations in normal form. The other two are

$$\dot{\Phi} = \Lambda + \mathcal{O}(\alpha) \tag{38a}$$

$$\dot{\Psi} = \lambda + \mathcal{O}(\alpha) \tag{38b}$$

It is very interesting that the *unaveraged* equation for $\dot{x}$ contains no periodic terms. If the transient terms discarded earlier had been included in the h_j, then, of course, *transient* periodic terms would appear.

First-Order Solution for the Nutation Angle Constant-Speed Rotor

The first-order solution for the nutation angle, in terms of x, may be developed by applying the generalized method of averaging to Eqs. (37) and (38).

Referring to the procedure in Ref. 9, the averaged $\dot{x}$ is equal to $\alpha A_1(\bar{x})$, where

$$A_1(\bar{x}) = \frac{1}{4\pi^2}\int_0^{2\pi}\int_0^{2\pi} X_1(x, \overline{\Phi}, \overline{\Psi})\,d\overline{\Phi}\,d\overline{\Psi} \tag{39}$$

and

$$X_1(x,\Phi,\Psi) = -\mu_P z^2\Lambda - \mu_R z^2(\Lambda + \dot{\phi}) \tag{40}$$

Since X_1 does not contain terms periodic in Φ of Ψ, the averaged equation for x, to first order in the small parameter α, is

$$\dot{\bar{x}} = -\alpha \bar{z}^2[\mu_P \bar{\Lambda} + \mu_R(\bar{\Lambda} + \dot{\phi})] \tag{41}$$

where $\bar{z}$ and $\bar{\Lambda}$ are obtained by replacing x with $\bar{x}$ in z and Λ, respectively.

For the case of a *constant-speed* rotor, Eq. (41) may be solved exactly by separating variables and using partial fractions. To make the equation for $\bar{x}$ simpler, some additional substitutions are necessary. First, we approximate $\bar{\Lambda}$ by using

$$\bar{\Lambda} = (H\bar{x} - \bar{h})/J_P - H\bar{x}/I_t \tag{42}$$

and use $h = J_R(\omega_2 + \dot{\phi})$. Second, we use the zeroth-order approximation to ω_3, i.e., $\omega_3 \simeq (H_3 - h)/J_P$, to write

$$\bar{h} = \frac{(H\bar{x} + J_P\dot{\phi})J_R}{J_P + J_R} + \mathcal{O}(\alpha) \tag{43}$$

Third, the above expression for $\bar{h}$ may be substituted into Eq. (42) to get

$$\bar{\Lambda} = \frac{\lambda\bar{x}(1-\sigma-\rho) - \dot{\phi}\sigma}{\sigma+\rho} \tag{44}$$

where $\sigma = J_R/I_t$ and $\rho = J_P/I_t$.

When Eq. (44) is used in Eq. (41), we obtain

$$\dot{\bar{x}} = \frac{\alpha\bar{z}^2[(\mu_P+\mu_R)(\sigma+\rho-1)\lambda\bar{x} + \dot{\phi}(\mu_P\sigma - \mu_R\rho)]}{(\sigma+\rho)} \tag{45}$$

Equation (45) may be rewritten in the concise form,

$$\dot{\bar{x}} = (1-\bar{x}^2)(a+b\bar{x}) \tag{46}$$

where

$$a = \frac{\alpha\dot{\phi}(\mu_P\sigma - \mu_R\rho)}{(\sigma+\rho)} \tag{47a}$$

and

$$b = \frac{\alpha\lambda(\mu_P+\mu_R)(\sigma+\rho-1)}{(\sigma+\rho)} \tag{47b}$$

By separating variables, using partial fractions and integrating Eq. (47) with $\bar{x} = \bar{x}_0$ at $t = 0$, we obtain the following implicit solution for $\bar{x}$:

$$t = -C_1 \ln\left(\frac{(1-\bar{x})}{(1-\bar{x}_0)}\right) + C_2 \ln\left(\frac{1+\bar{x}}{1+\bar{x}_0}\right) + C_3 \ln\left(\frac{a+b\bar{x}}{a+b\bar{x}_0}\right) \tag{48}$$

where

$$C_1 = 1/[2(a+b)] \tag{49a}$$

$$C_2 = 1/[2(a-b)] \tag{49b}$$

$$C_3 = b/(a^2-b^2) \tag{49c}$$

Stability Criteria for the Constant-Speed Rotor Case

If the spacecraft's nominal attitude motion of steady spin is asymptotically stable in the sense that the nutation angle approaches zero, then the average value of the nutation angle must also approach zero. This *does not* necessarily mean, if our approximation to the nutation angle approaches zero, that the spacecraft's nominal attitude motion is asymptotically stable with respect to perturbations in nutation. However, since our equation for $\bar{x}$ is valid for sufficiently small α, it should correctly predict stability when α is very small. Thus, although criteria based on the approximate equation for $\cos\Theta = x$ are not to be considered *exact*, they should prove very useful when applied with their limitations in mind.

To obtain stability criteria, we consider the requirements for $\bar{x} \to 1$ as $t \to \infty$. This will occur if $\dot{\bar{x}} > 0$, for $0 < \bar{x} < 1$, Hence, we want

$$(1-\bar{x}^2)(a+b\bar{x}) > 0, \qquad 0 < \bar{x} < 1 \tag{50}$$

Since

$$(1-\bar{x}^2) > 0 \text{ for } 0 < \bar{x} < 1 \tag{51}$$

if we require that

$$a + b\bar{x} > 0, \qquad 0 < \bar{x} < 1 \tag{52}$$

then $\bar{x}$ will approach unity.

Regarding the motion predicted by Eq. (46), three equilibrium points are mathematically possible: $\bar{x}_e = 1$, -1, and $-(a/b)$. Physically, $\bar{x}_e = -(a/b)$ is of interest only if $|a/b| < 1$. Equation (46) may be linearized about $\bar{x}_e = 1$ to obtain the equation, $\Delta\dot{x} = -2(a+b)\Delta x$, where $\Delta x \triangleq \bar{x} - \bar{x}_e$. Hence, the nutational motion predicted by Eq. (46) is asymptotically stable if $a + b > 0$ and the initial value of $\bar{x}$, say $\bar{x}_0$, is sufficiently close to 1. Similarly, the point $\bar{x}_e = -1$ (or $\Theta = \pi$) is asymptotically stable when $a - b < 0$ and $\bar{x}_0$ is sufficiently close to -1.

The issue of whether the points $\bar{x}_e = 1$ and $\bar{x}_e = -(a/b)$ can be asymptotically stable at the same time naturally arises. Since we are only concerned about $\bar{x}_e = -(a/b)$ when $0 < -(a/b) < 1$ and since the point $\bar{x}_e = -(a/b)$ is asymptotically stable only if $b < 0$, we have $a < -b$ and hence $a + b < 0$. Therefore, the points *are not* simultaneously asymptotically stable. If $a < 0$, $b > 0$, and $-(a/b) < 1$, then for $\bar{x}_0 < -(a/b)$, $\bar{x} \to -1$ as $t \to \infty$ even though $a + b > 0$.

Table 1 provides a summary of the possible cases and the corresponding stability characteristics of the most important equilibrium point, $\bar{x}_e = 1$, which corresponds to $\Theta = 0$.

Table 1 Nutational stability about $\Theta = 0$ for a spacecraft with a constant-speed rotor

	Case	Asymptotically stable	Unstable
I	$a > 0,\ b > 0$	X	
II	$a > 0,\ b = 0$	X	
III	$a > 0,\ b < 0$		
	(1) $\lvert a/b\rvert > 1$	X	
	(2) $\lvert a/b\rvert < 1$		X
IV	$a = 0,\ b > 0$	X	
V	$a = 0,\ b = 0$	Neutrally stable	
VI	$a = 0,\ b > 0$		X
VII	$a < 0,\ b > 0$		
	(1) $\lvert a/b\rvert > 1$		X
	(2) $\lvert a/b\rvert < 1,\ 1 > x_0 > -a/b$	X	
	(3) $\lvert a/b\rvert < 1,\ -a/b > \bar{x}_0$		X
VIII	$a < 0,\ b = 0$		X
IX	$a < 0,\ b < 0$		X

Small Nutation Angles

For the case of a *despun platform* in which the spherical body in the rotor is rotating with it, *initially* $H_{30} = (J_R + I_R)\dot{\phi}$ and $x_0\lambda = H_{30}/I_t = \sigma^*\Omega$, where $\sigma^* = \sigma + \alpha$. *If the nutation angle remains small*, then these conditions should continue to be very nearly satisfied and Eq. (52) can be replaced by $a + b > 0$ or

$$\mu_P(\sigma + \rho - 1 + \sigma/\sigma^*) + \mu_R(\sigma + \rho - 1 - \rho/\sigma^*) > 0 \quad (53)$$

We note that if $\mu_R = 0$, the criterion for asymptotic stability is $\sigma + \rho + \sigma/\sigma^* > 1$. For small α, $\sigma/\sigma^* \simeq 1$ and the criterion is satisfied for all σ and ρ. Since $\mu_R = 0$ implies energy dissipation on only the despun platform, the nutational motion should be asymptotically stable.[2]

When $\mu_P = 0$ and α is small, the criterion is

$$\sigma + \rho - 1 - \rho/\sigma^* > 0$$

which reduces to

$$\sigma + \rho > (\sigma + \rho)/\sigma \quad (54)$$

The inequality equation (54) is satisfied if $\sigma > 1$, i.e., if the rotor is oblate. More generally, Eq. (54) is satisfied if

$$\sigma > \frac{1-\rho}{2} + \sqrt{\frac{(1-\rho)^2}{4} + \rho} \quad (55)$$

Stability Diagrams for Small Nutation Angles

The left-hand side of the inequality equation (53) is a function of δ_P, δ_R, λ, σ, ρ, and α. If the small angle approximation $\lambda = \sigma^*\Omega$ is used in the expressions for μ_P and μ_R, then Eq. (53) can be rewritten and multiplied by Ω to get

$$\frac{(\delta_P/\Omega)(\sigma + \rho - 1 + \sigma/\sigma^*)}{(\delta_P/\Omega)^2 + \sigma^{*2}} + \frac{(\delta_R/\Omega)(\sigma + \rho - 1 - \rho/\sigma^*)}{(\delta_R/\Omega)^2 + \sigma^{*2}} > 0 \quad (56)$$

By first specifying α, ρ, and σ, we can then use inequality equation (56) to delineate stable and unstable regions of the $(\delta_P/\Omega)(\delta_R/\Omega)$ plane. Figures 3-5 are examples of stability diagrams obtained in this manner.

Figure 3 illustrates the case of equal spin axis moments of inertia of the rotor and platform. Because $\alpha \neq 0$, the stability boundaries do not intersect at exactly (0.5,0.5). A value of $\rho > \sigma$ with $\rho + \sigma > 1$ produces separated unstable regions and a large stable region. The stability boundaries separate in the *vertical* direction when $\sigma > \rho$.

The stability diagrams given in Figs. 3-5 are very similar to certain diagrams given in Ref. 4 and based on a linear stability analysis that is exact in a region about the equilibrium state corresponding to steady spin. Here, the analysis is approximate in the sense that the effects of the damper must be "small," but the stability criterion involves both rotor and platform inertia parameters and the effect of the inertia of the damper contained in the rotor. The linear analysis[4] did not provide information about the platform inertia parameters.

Large Nutation Angles

In addition to the foregoing stability diagrams and others that may be obtained from Eq. (56), we may use the solution for $\bar{x}$ to predict nutational motion. Figures 6-8 show examples of the nutation angle time histories obtained by numerically integrating the exact equations of motion using a fourth-order Runge-Kutta algorithm and Eq. (48). Each of the time histories was generated using $\dot{\phi} = \Omega = 1$ rad/s and $\omega_{10} = 0.2$ rad/s, with all other initial conditions zero. There is very good agreement between the exact and approximate solutions even though both α and Θ_0 are fairly large.

An interesting aspect of the approximate equation for cos Θ is that, in motion corresponding to case III, for $|a/b| < 1$, $\bar{x} \to -a/b$ as $t \to \infty$. In order to verify this, the exact equations were integrated using $\alpha = 0.01$, $\delta_P = 1.8$, $\delta_R = 1.6$, $\sigma = 0.5$, $\rho = 0.4$, $\omega_{10} = 0.10$ rad/s, $\omega_{20} = \omega_{30} = 0$, $\dot{\phi} = 1$ rad/s, and zero relative angles rates of all the dampers. For these data, $a \simeq 1.515 \times 10^{-4}$ rad/s, $\bar{x}_0 = 0.9798$, and $\Theta_0 = 11.53$ deg. The equilibrium angle $\bar{\Theta}_e = \cos^{-1}[-a/b] = 60.14$ deg is predicted by Eq. (46). The numerical integration yielded a limiting angle of approximately 65 deg.

In case VII(3), large-amplitude motion should be unstable, while small-amplitude motion is asymtotically stable in case VII(2). As a test of these results, the values $\alpha = 0.01$, $\delta_P = 1.0$, $\delta_R = 1.0$, $\sigma = 0.5$, $\rho = 0.6$, $\omega_{10} = 0.05$ rad/s, $\dot{\phi} = 1$ rad/s, and all other initial conditions zero were used to obtain a time history of Θ. For these values, $a = -3.69 \times 10^{-3}$ rad/s, $b = 3.782 \times 10^{-3}$ rad/s, $\bar{\Theta}_e = 12.69$ deg, and $\bar{\Theta}_0 = 5.66$ deg;

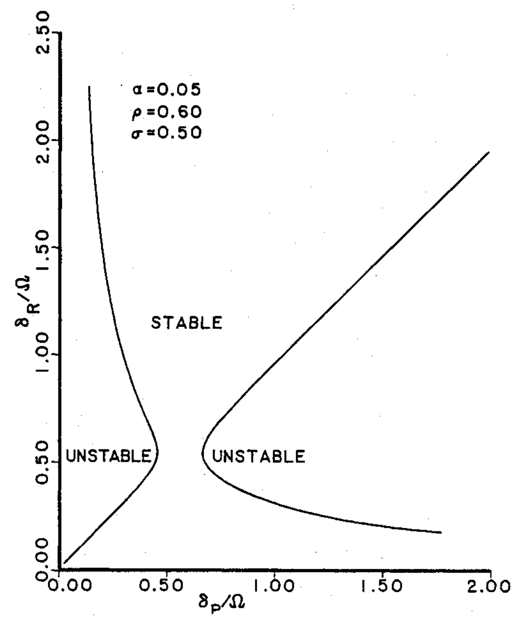

Fig. 4 Stability diagram for α = 0.05, ρ = 0.6, and σ = 0.5.

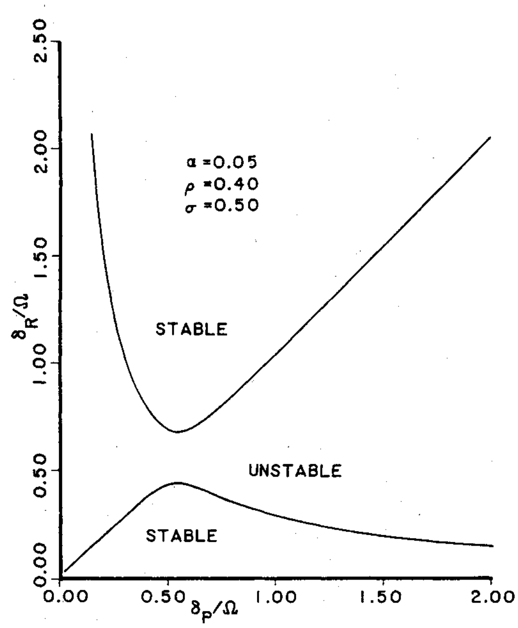

Fig. 5 Stability diagram for α = 0.05, ρ = 0.4, and σ = 0.5.

hence, the nutational motion should be stable. Numerical results are in agreement. For the same initial conditions except $\omega_{10} = 0.2$ rad/s and $\omega_{30} = -0.03558$ rad/s, $\Theta_0 = 23.46$ deg $> \bar{\Theta}_e$. For such an initial Θ, unstable motion is expected and has been found using the exact equations.

Effects of a Free Rotor

When the speed of the rotor is not controlled and there is no friction between the platform and rotor, simulated behavior of the spacecraft for large nutation angles has indicated that an apparent "reversal" of nutational stability may occur. Although the free-rotor case is not of as much general interest as the constant-speed rotor case, the free-rotor case should be considered because of these rather anomalous results and because there is at least one set of circumstances in which the free-rotor condition may be of practical interest. These circumstances are a failure of the motor that maintains $\dot{\phi} = \text{const}$ when there is some nutational motion. The attitude behavior of the spacecraft following such a failure may be very important. It may, for example, terminate in tumbling motion of the spacecraft about an axis orthogonal to the original spin axis.

Because the rotor and damper together are symmetric about the x_3 axis, in the case of a free rotor, the time rate of change of the x_3 component of angular momentum of the rotor and damper together is given by

$$\frac{d}{dt}[J_R(\omega_3 + \dot{\phi}) + I_R(\omega_3 + \dot{\phi} + \omega_{R3})] = I_R(\omega_{R2}\omega_1 - \omega_{R1}\omega_2) \tag{57}$$

Also, the time rate of change of the x_3 component of the angular momentum of the damper in the rotor is

$$\frac{d}{dt}[I_R(\omega_3 + \dot{\phi} + \omega_{R3})] = -C_R\omega_{R3} + I_R(\omega_{R2}\omega_1 - \omega_{R1}\omega_2) \tag{58}$$

By subtracting Eq. (58) from Eq. (57), we get

$$\frac{d}{dt}[J_R(\omega_R + \dot{\phi})] = C_R\omega_{R3} \tag{59}$$

In an equilibrium state, the damper must rotate with the rotor. Thus, we introduce the dimensionless variable, $x_2 \triangleq (I_R + J_R)(\omega_3 + \dot{\phi})/H$. Then, from Eq. (59), we have

$$\dot{x}_2 = \frac{[(I_R + J_R)/J_R]C_R\omega_{R3}}{H} \tag{60}$$

Equation (2c) provides $\omega_{R3} = h_{R3}/I_R - (\omega_3 + \dot{\phi})$. The approximation $\omega_3 \simeq (H_3 - Hx_2)/J_R$ and the zeroth-order solution for H_{R3} given by Eq. (32c) can then be used in Eq. (60) to get the *averaged* equation,

$$\dot{\bar{x}}_2 = (1 - \bar{x}_1^2)(c_3\bar{x}_1 + c_4\bar{x}_2) \tag{61}$$

where

$$c_3 = \alpha[\delta_R\lambda^2/(\delta_R^2 + \lambda^2)] = \alpha_R \tag{62a}$$

and

$$c_4 = -\alpha_R/\sigma \tag{62b}$$

Here, $\alpha_R = \alpha\lambda\mu_R$ and we have, for convenience, put $\bar{x}_1 = \bar{x}$.

We may also rewrite Eq. (46) for $\bar{x} = \bar{x}_1$, by using $\bar{x}_2$ to replace the *now variable* $\dot{\phi}$, in the form,

$$\dot{\bar{x}}_1 = (1 - \bar{x}_1^2)(c_1\bar{x}_1 + c_2\bar{x}_2) \tag{63}$$

where

$$c_1 = \alpha_R + \alpha_P - \alpha_P/\rho \tag{64a}$$

and

$$c_2 = \alpha_P/\rho - \alpha_R/\sigma \tag{64b}$$

with $\alpha_P = \alpha\lambda\mu_P$.

Equations (61) and (63) can, in principle, be reduced to quadrature.[10] However, the solution is complicated and not immediately informative. We chose therefore to investigate the stability of the average motion described by Eqs. (61) and (63) using phase-plane diagrams, or "phase paths" (see Ref. 10, pp. 86-90, and Ref. 11, pp. 59 and 65).

We may express Eqs. (61) and (63) in the forms,

$$\dot{\bar{x}}_1 = P(\bar{x}_1, \bar{x}_2) \tag{65a}$$

and

$$\dot{\bar{x}}_2 = Q(\bar{x}_1, \bar{x}_2) \tag{65b}$$

respectively. The equilibrium points of Eqs. (65) are (0,0) and the *lines* $\bar{x}_1 = \pm 1$. Since $\bar{x}_1 = 1$ corresponds to $\bar{\Theta} = 0$, we will not consider the line $\bar{x}_1 = -1$ (which corresponds to $\bar{\Theta} = \pi$). Also, although $\bar{x}_2$ may be negative, in the most interesting case, namely, nutational stability of the spacecraft when $\dot{\phi} \geq 0$

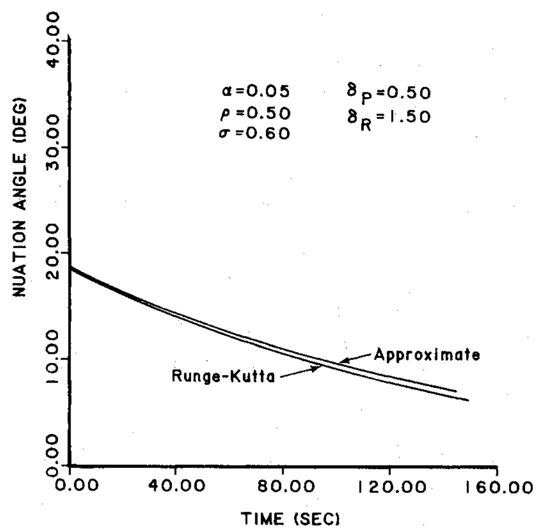

Fig. 6 Exact and approximate nutation angle time histories for $\rho < \sigma$ and $\delta_P < \delta_R$.

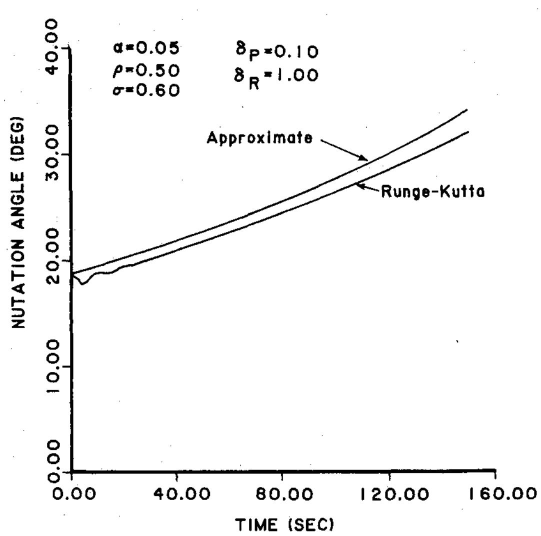

Fig. 7 Exact and approximate nutation angle time histories for $\rho < \sigma$ and $\delta_P \ll \delta_R$.

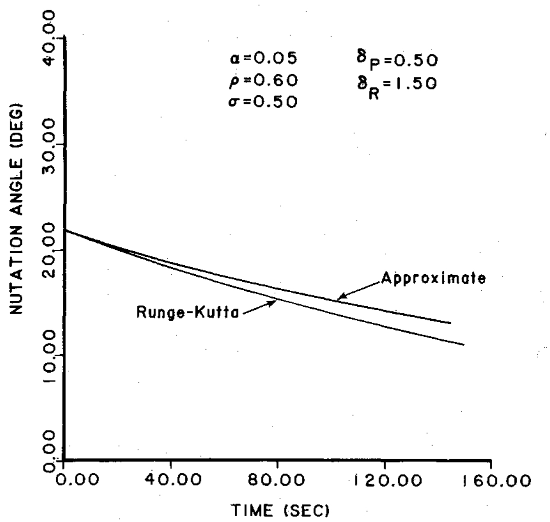

Fig. 8 Exact and approximate nutation angle time histories for $\rho < \sigma$ and $\delta_P < \delta_R$.

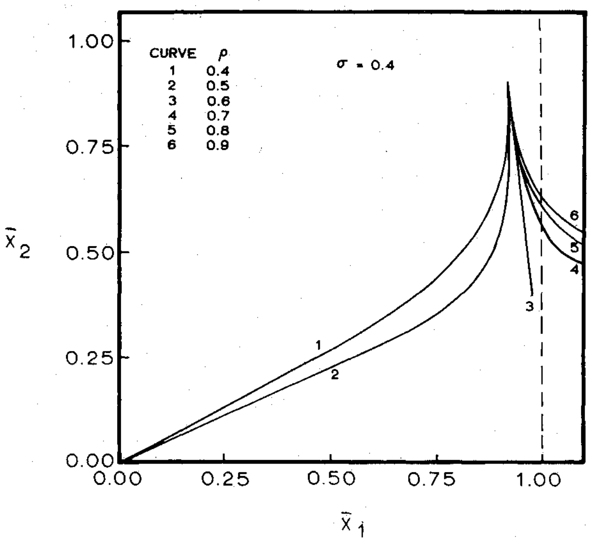

Fig. 9 Phase plane diagram: effects of varying ρ.

and $\bar{\omega}_3 \geq 0$, $0 \leq \bar{x}_2 \leq 1$. Therefore, we will not consider the case $\bar{x}_2 < 0$ here.

To obtain phase paths, we introduce the arc length $ds = \sqrt{P^2 + Q^2}\, dt$ and get the equations,

$$\frac{d\bar{x}_1}{ds} = \frac{(c_1\bar{x}_1 + c_2\bar{x}_2)}{D} \tag{66a}$$

and

$$\frac{d\bar{x}_2}{ds} = \frac{(c_3\bar{x}_1 + c_4\bar{x}_4)}{D} \tag{66b}$$

where $D = [(c_1\bar{x}_1 + c_2\bar{x}_2)^2 + (c_3\bar{x}_1 + c_4\bar{x}_2)^2]^{\frac{1}{2}}$. Note that when ds is introduced, the line of equilibrium points no longer appears directly. Also, since α is a multiplicative factor of each of the c_j, $j = 1,2,3,4$, we can put $\alpha = 1$ in computing phase paths.

Before we discuss specific results, we note that, if c_1 and c_2 are of opposite signs, then $d\bar{x}_1/ds$ will change sign when $\bar{x}_2 = -(c_1/c_2)\bar{x}_1$, provided $c_3\bar{x}_1 + c_4\bar{x}_2 \neq 0$ also, which would require that $c_1c_4 - c_2c_3 = 0$. If, with the equilibrium points on the line segment $\bar{x}_1 = 1$, $0 < \bar{x}_2 < 1$, disregarded, the change of sign in $d\bar{x}_1/ds$ occurs for $\bar{x}_1 > 1$; and if $d\bar{x}_1/ds > 0$ at the

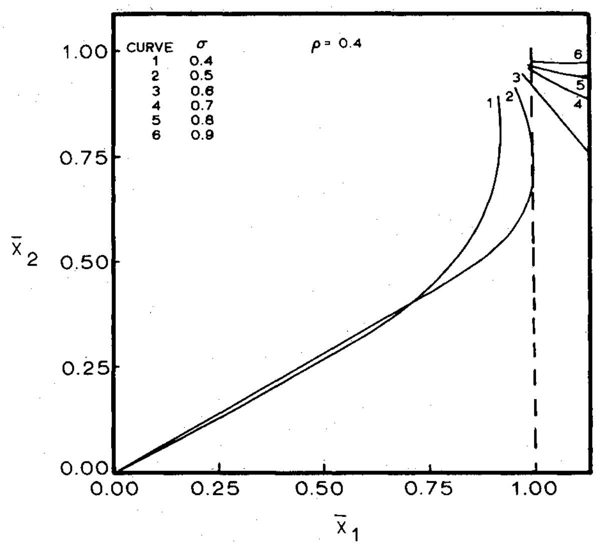

Fig. 10 Phase plane diagram: effects of varying σ.

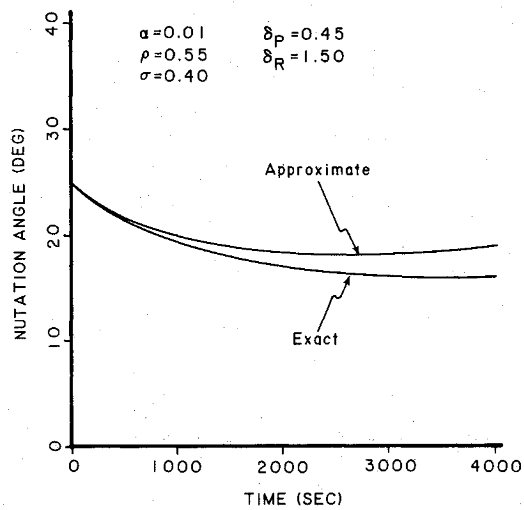

Fig. 11 Exact and approximate nutation angle time histories for free-rotor example.

initial point, then $\bar{x}_1$ will approach 1. When $\omega_{30} = 0$, $\bar{x}_{10} = \bar{x}_{20}$. Also, since $c_3 > 0$, for $\sigma < 1$, $c_4 < -\bar{c}_3$ and x_2 will decrease. Thus, for stable nutational motion we must certainly have $0 \leq -c_1/c_2 <$ (minimum expected value of $\bar{x}_2$).

Figure 9 shows a phase plane diagram for the parameter values, $\sigma = 0.4$; $\rho = 0.4, 0.5, 0.6, 0.7$; $\delta_P = 0.45$; and $\delta_R = 1.5$ and starting values of $\bar{x}_1$ and $\bar{x}_2$ corresponding to $\omega_{10} = 0.1875$ rad/s, $\omega_{20} = \omega_{30} = 0$, and $\dot{\phi}_0 = 1.0$ rad/s. For $\rho > 0.6$, $\bar{x}_1$ and $\bar{x}_2$ approach zero. For $\rho = 0.6$, $c_1c_4 - c_2c_3 = 0$ and the phase point *stops* when $\bar{x}_2 = -(c_1/c_2)\bar{x}_1$.

A similar, but different set of curves is shown in Fig. 10. The parameter varied to get these curves is σ. The initial points are not all the same because a change in σ produces a change in H_{30} and, hence, H and $\cos\bar{\Theta}_0$. The curve for $\sigma = 0.6$ and $\rho = 0.4$ terminates in the region to the right of $\bar{x}_1 = 1$. Thus, for $\sigma = 0.6$ and $\rho = 0.4$, the nutational motion is asymptotically stable. The curve for $\sigma = 0.5$ just crosses the line $\bar{x}_1 = 1$. Hence, we could expect that for that case, $\bar{\Theta}$ also approaches zero. "Exact" time histories have been obtained that support this conclusion. When $\sigma < 0.5$, the "turning point" (point at which $d\bar{x}_1/d\bar{x}_2 = 0$) occurs for $\bar{x}_1 < 1$ and $\bar{x}_1$ and $\bar{x}_2$ both go to zero.

Time histories of Θ and $\bar{\Theta}$ for a case in which $\dot{\Theta}$ reverses sign are shown in Fig. 11. These results were obtained using the following data: $\alpha = 0.01$, $\rho = 0.55$, $\sigma = 0.40$, $\delta_P = 0.45$, $\delta_R = 1.5$, $\omega_{10} = 0.1875$ rad/s, $\omega_{20} = \omega_{30} = 0$, and $\dot{\phi}_0 = 1$ rad/s.

For this example, $c_1 = -0.0006$ rad/s, $c_2 = 0.000986$ rad/s, $c_3 = 0.001251$ rad/s, and $c_4 = -0.003127$ rad/s. The approximate solution remains very close to the exact solution for 4000 s. The corresponding phase plane diagram indicates that $\dot{\Theta}$ should at first be negative, but should later reverse sign. This reversal does in fact occur at around $t = 3550$ s. Generally, for α reasonably small, the approximate solution correctly predicts whether or not the nutational motion is asymptotically stable.

Conclusions

The attitude motion of a model of a symmetric dual-spin spacecraft containing spherical dampers within both its rotor and platform has been investigated. A perturbation method that treats the effects of the motion of the dampers as perturbing torques has been used in conjunction with the generalized method of averaging. The use of the perturbation method is somewhat more complicated than a standard linear analysis of the nominal steady spin state. However, since small angles are not required for application of the perturbation method, the results obtained provide useful information concerning nonlinear attitude motion of the spacecraft.

A stability analysis, conducted for the constant-speed rotor case assuming small nutational angles, produced results that agree well with those of linear stability analyses. The analysis of this paper differs from a linear analysis in that more information regarding the inertia parameters is embodied in the stability criterion than in a conventional linear criterion. More importantly, the generalized method of averaging provides an approximate solution for nutational motion that is not restricted to small angles. Results obtained from this solution agree well with results obtained by numerically integrating the full set of nonlinear equations. For a constant-speed rotor, the *linear* stability criterion is valid for large nutational angle motion, with one exception.

It was shown that, when the effects of a free rotor on the attitude stability are considered, the approximate equations may be used successfully to predict reversals of the rate of change of the nutation angle which may occur under certain conditions. Although no explicit stability criterion was obtained for the free-rotor case, the use of the approximate equations to generate phase-plane diagrams from which stability characteristics can be inferred was illustrated.

Appendix

Zeroth-order approximations to the ω_k, $k = 1,2,3$, may be derived from Eqs. (5), (13), (17a), and (17b). Since the h_j, $j = 1, 2, 3$, are first-order terms, the zeroth-order approximations to Eqs. (5) are

$$\omega_1 \simeq H_1/I_t \tag{A1a}$$

$$\omega_2 \simeq H_2/I_t \tag{A1b}$$

and

$$\omega_3 \simeq (H_3 - h)/J_P \tag{A1c}$$

where the H_j are given by Eqs. (13) with Eqs. (17a) and (17b) used to approximate Θ and Φ. Hence, for the constant-speed rotor case, we have

$$\omega_1 \simeq (H/I_t)\sin\Theta_0\sin(\Lambda t + \Phi_0) \tag{A2a}$$

$$\omega_2 \simeq (H/I_t)\sin\Theta_0\cos(\Lambda t + \Phi_0) \tag{A2b}$$

$$\omega_3 \simeq (H/J_P)\cos\Theta_0 - h/J_P \tag{A2c}$$

Acknowledgments

The first author wishes to acknowledge the support of the U.S. Air Force during his graduate work and both authors acknowledge the assistance provided by Mr. Brian S. Lahr, the expert typing of the manuscript by Mrs. Marjorie McGee, and the many constructive suggestions of the reviewers.

References

[1] Kaplan, M.H., *Modern Spacecraft Dynamics and Control*, John Wiley & Sons, New York, 1976, Chaps. 2 and 5.

[2] Landon, V.D. and Stewart, B., "Nutational Stability of an Axisymmetric Body Containing a Rotor," *Journal of Spacecraft and Rockets*, Vol. 1, Nov.-Dec. 1964, pp. 682-684.

[3] Likins, P.W., "Attitude Stability Criteria for Dual-Spin Spacecraft," *Journal of Spacecraft and Rockets*, Vol. 4, Dec. 1967, pp. 1638-1643.

[4] Laskin, R.A., Sirlin, S., and Likins, P.W., "Stability of a Dual-Spin Spacecraft with Spherical Dampers," Paper presented at AAS/AIAA Astrodynamics Specialist Conference, Lake Placid, NY, Aug. 1983.

[5] Cochran, J.E. Jr. and Shu, P.H., "Nutational Motion of an Asymmetric Dual-Spin Spacecraft," Paper presented at AAS/AIAA Astrodynamics Specialist Conference, Lake Placid, NY, Aug. 1983.

[6] Meirovitch, L., *Methods of Analytical Dynamics*, McGraw-Hill Book Co. New York, 1970.

[7] Cochran, J.E. Jr., "Nonlinear Resonances in the Attitude Motion of Dual-Spin Spacecraft," *Journal of Spacecraft and Rockets*, Vol. 14, Sept. 1977, pp. 562-572.

[8] Etkin, B., *Dynamics of Atmospheric Flight*, John Wiley & Sons, New York, 1972, pp. 118-119.

[9] Winfree, P.K., "Nonlinear Attitude Stability of a Dual-Spin Spacecraft Containing Spherical Dampers," Master of Science Thesis, Auburn University, Auburn, AL, June 1984.

[10] Jordan, D.W. and Smith, P., *Nonlinear Ordinary Differential Equations*, Clarendon Press, Oxford, England, 1977.

[11] Hahn, W., *Stability of Motion*, Springer-Verlag, New York, 1967.